Pol. J. Environ. Stud. Vol. XX, No. X (XXXX), 1-11
DOI: *10.15244/pjoes/203058* ONLINE PUBLICATION DATE: 2025-04-29

Original Research

Spatial and Temporal Patterns and Driving Factors of Desertification in Hulunbuir Grassland

Simiao Guan[1], Xiwei Zhang[1, 2]*, Nacun Batu[1], Mei Yong[1], Yu Chen[1], Tianqiao Zheng[1], Xin Guo[1], Yangyang Li[1]

[1]College of Geographic Sciences, Inner Mongolia Normal University, Hohhot 010022, China
[2]Land Use and Remediation Engineering and Technology Research Center of Inner Mongolia Autonomous Region, Hohhot 010022, China

Received: 29 August 2024
Accepted: 17 March 2025

Abstract

The Hulunbuir Grassland is located in the semi-arid region of northern China and is highly sensitive to environmental changes, with sandy inlays within the grassland and heavy desertification problems. However, there has been a lack of systematic research on the long-term distribution pattern of desertification and influencing factors. This study adopted the multi-indicator fusion desertification level extraction method to explore the temporal distribution characteristics, spatial distribution pattern, and desertification center of the gravity migration pattern of the Hulunbuir sands and applied the parameter optimal geographic detector to generate the optimal discretized factors from the continuous meteorological and topographical factors to detect the main driving factors and mechanism of desertification of Hulunbuir Grassland over its entire range. The results showed that the explanatory power of meteorological factors was significantly stronger than that of topographic factors in the entire area of Hulunbuir Grassland. Among meteorological factors, annual precipitation had the strongest explanatory power for desertification; meteorological and topographic factors were nonlinearly enhanced, and the interaction between precipitation and slope had the strongest explanatory power, indicating that the interaction between precipitation and slope influenced vegetation and soil humidity and thus indirectly influenced the desertification evolution process.

Keywords: desertification, spatial and temporal patterns, driving factors, parameter-optimized geoprobe, Hulunbuir grassland

Introduction

Desertification is a typical feature of land degradation processes in extremely arid, arid, semi-arid, and partially semi-humid areas[1] and induces dust storms and sandstorms, which affect human socioeconomic activities. According to the National Bulletin of Desertification Situation (2013-2015), the total area affected by desertification in China is 1,721,200 km^2, which is mainly distributed in agricultural and pastoral intertwined zones in the northern arid, semi-arid, and semi-humid zones, particularly in the Inner Mongolia Autonomous Region, accounting for 34.5% of the total

*e-mail: zhangxw@imnu.edu.cn
Tel.: +86-15754841007

area. Desertification leads to loss of soil organic matter and fine-grained material, soil coarsening, and sand and dust storms, and gradually manifests as degradation of vegetation cover, a declining water table, declining soil fertility, and reduced net primary productivity (NPP) [2]. Regarding soil texture, the soil sand content in the study area is high and mostly medium and fine sand, coupled with interferences from human activities (particularly irrational use of soil and water resources), which seriously restrict the ecological security and sustainable socioeconomic development of the region [3].

At present, long-term monitoring data of desertification in Hulunbuir Grassland are limited; in particular, high-resolution spatial and temporal data are lacking, making it difficult to accurately describe the dynamic process of desertification. Thus, spatial heterogeneity of the desertification degree and its change pattern in different regions has not been adequately analyzed, and the characteristics of the evolution of desertification in different geographic units have not been comprehensively revealed. Therefore, the uncertainty of the long-term spatial and temporal evolutionary characteristics of desertification in Hulunbuir Grassland and the unclear mechanisms of climate change and topographic factors have become problems that need to be solved urgently. In view of this, this study extracted desertification information with a multi-indicator desertification hierarchical classification system, analyzed the spatial and temporal patterns of desertification, applied the parameter-optimal geoprobe model, and selected the parameter combinations with the highest q-value to generate the optimal discretization factors for the continuous meteorological and topographical factors [1]. We also detected the main drivers of desertification of Hulunbuir Grassland and their spatial variations to provide references for early warning, prediction, zoning prevention, and control of desertification of Hulunbuir Grassland. This study plays an important role in the area's ecological protection and sustainable development, as well as in developing an early warning system for desertification.

Materials and Methods

Study Area

Hulunbuir Grassland is located in the northeast of the Inner Mongolia Autonomous Region and the west of Daxinganling (47°08'–53°23'N, 115°22'–126°06'E) [4] and is one of the four major sandy areas in China. The study area included two districts (Hailar and Jalainur) and five flag counties (Chen Barag Banner, Xin Barag Right Banner, Xin Barag Left Banner, Ewenke

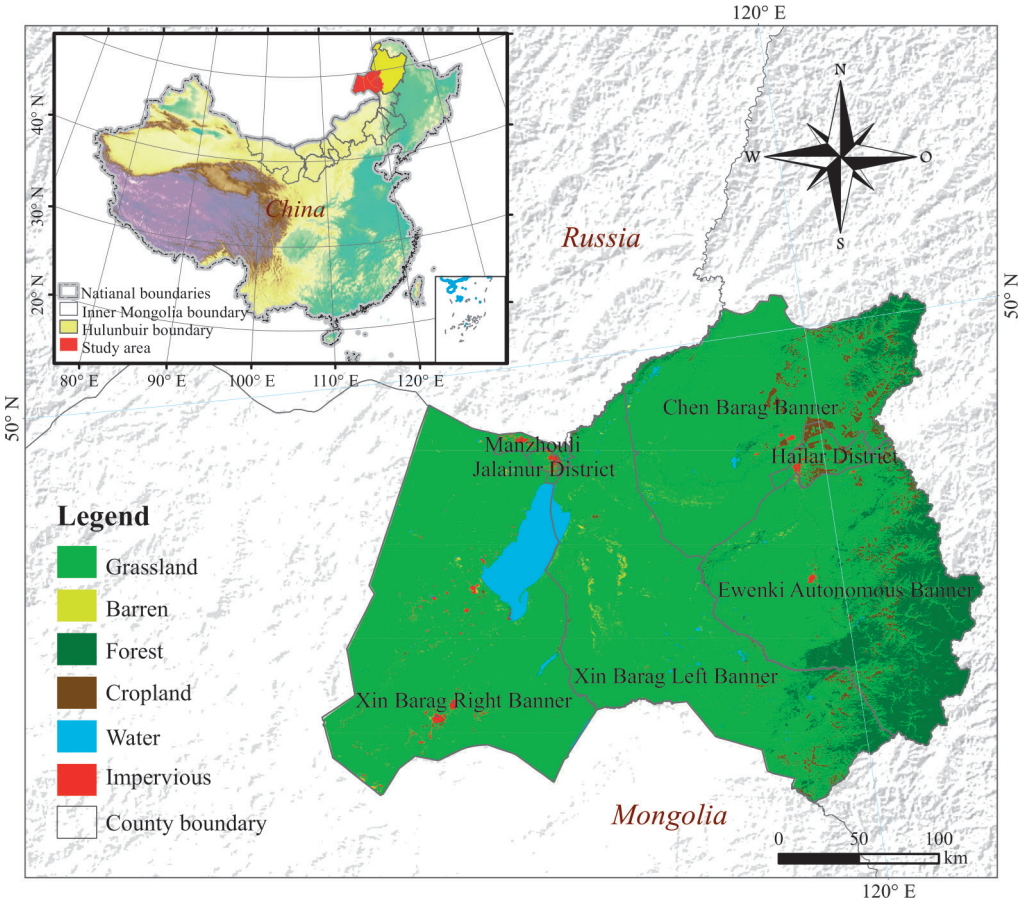

Fig. 1. Geographical location and land use/cover map of Hulunbuir Sandy Land in 2020.

Autonomous Banner, and Manzhouli), covering an area of approximately 83,095 km² (Fig. 1) [5]. Water resources are extremely rich, with >3,000 rivers of different sizes and 300 lakes. The terrain is high in the east and low in the west. From east to west, it gradually transitions from a forest area to a grassland area, with an altitude of approximately 700 m above sea level. The study area has a temperate continental climate and is located in the semi-arid and semi-humid transition zone [6], with regional annual precipitation of 280-500 mm, >70% of which occurs from July-September, an average annual temperature of 2.2-4.3°C, abundant sunshine, and annual evaporation of 1100-1700 mm. Since extreme climate occurred in the study area in 2016, including a sharp drop in precipitation and a sharp rise in temperature, the trend in the desertification area changed from decreasing to increasing, and the sand control project has been hindered [7]. Sand and dust storms occur for approximately 3-10 day/s [8], and desertification is an extremely serious problem.

Data Sources and Research Methodology

Data Sources

Meteorological data were obtained from six meteorological stations in Hulunbuir City, all of which originated from the China Meteorological Data Service Center (http://data.cma.cn) and included annual precipitation and annual mean temperature data from 2000-2020. Digital elevation model (DEM) data were used to generate slope and slope direction data in the study area; DEM data were 90 m SRTMDEM (SRTM3V4.1) images (http://srtm.csi.cgiar.org/). Remote-sensing data were obtained from Landsat satellites (ETM+, TM, and OLI), originating from the Google Earth Engine cloud platform, and included five views of images in 2000, 2005, 2010, 2015, and 2020, with 30×30-m spatial resolution, cloudiness of <5%, and during July when the forest and grass vegetation were in an optimal growth condition. Land-use data were obtained from the "CLCD land cover dataset" published by the team of Profs. Yang Jie and Huang Xin from Wuhan University [9]. The temperature-vegetation drought index model was used to invert soil moisture.

Multi-Indicator Fusion Desertification Information Extraction Method

The desertification class classification method proposed by WANG Shuxiang [10] was adopted based on the traditional fractional vegetation cover (FVC) classification method, the modified soil-adjusted vegetation index (MSAVI), and the enhanced vegetation index (EVI), which effectively solves the shortcomings of the traditional method of low differentiation between grades and improves the accuracy of land classification (Table 1). The improvement in the extraction accuracy of desertification data mainly used a combination of field validation and Google Earth high-resolution images [11], and the data accuracy evaluated using the confusion matrix was >90%.

Spatial Autocorrelation

This method assumes a certain similarity or dependence between data values in spatially adjacent or similar locations, which should weaken with increasing distance until it disappears. It is divided into two types: global spatial autocorrelation and local spatial autocorrelation. Spatial autocorrelation, which reflects the spatial distribution status of desertification, utilized global autocorrelation [7] to describe the correlation between desertification grids in the Hulunbuir Grassland and to assess the pattern of desertification in a discrete, random, or agglomerated pattern. Local autocorrelation was utilized to measure the degree of correlation between the local and surrounding areas. This study adopted the LISA diagram to reflect the spatial autocorrelation in the local area, which was classified into high-high (H-H), high-low (H-L), and low-high (L-H), and three types of agglomeration.

Standard Deviation Ellipse Model (SDE)

This method was used to measure the directional distribution of desertification, obtain the distribution

Table 1. Desertification classification standards.

Desertification level	Condition		Features
Non-desertification	FVC≥0.6	MSAVI≥0.1	Basically, there's no wind-blown sand activity, mainly a large area of cultivated land; the morphological characteristics of farmland are obvious, and the proportion of bare sand area is very small.
Mild desertification	FVC≥0.6	MSAVI<0.1	Less wind and sand activity, no obvious dune morphology, and more vegetation, but its distribution is discontinuous.
Moderate desertification	FVC<0.6	EVI≥0.25	Frequent wind and sand activities, and the sand dunes are in the form of strips or irregular patches, alternating with sparse vegetation.
Heavy desertification	FVC<0.6	EVI<0.25	Violent aeolian sand activity and the morphological characteristics of the sand dunes are clear, with an obvious wave-like texture and almost no vegetation distribution.

direction of desertification, and elucidate spatial characteristics such as the degree of dispersion and directional trend. Specifically, the direction of the long half-axis of the ellipse represented the direction of desertification distribution, the length of the short half-axis of the ellipse represented the range of desertification distribution, and the difference between the lengths of the long and short axes represented the flatness of the ellipse. The larger the difference, the stronger the directionality, and the size of the ellipse represented the degree of concentration of the historical spatial pattern of desertification. In summary, this method provided a quantitative and systematic method for analyzing desertification spatial patterns and an effective method for desertification detection and management.

Parameter-Optimized Geoprobes

Geodetectors [12] can detect and analyze the driving factors of desertification, such as topographic and meteorological factors, to determine the spatial differentiation of desertification and reveal its main driving forces. However, traditional geographic detectors need to be set arbitrarily when discretizing continuous variables, and there are problems such as subjectivity and poor discretization. Therefore, the optimal parameters-based geographical detector [13] (OPGD) was selected to analyze the desertification driving force in Hulunbuir Grassland in this study.

Based on previous studies [14, 15], soil moisture, elevation, slope, slope direction, distance from roads, distance from settlements, and distance from water bodies were selected as topographic factors, and precipitation and air temperature were selected as meteorological factors. All the above factors were continuous. The q-value of each continuous factor was calculated under different grading methods and different numbers of breaks and was in the interval of [0-1]; the larger the value, the stronger the spatial differentiation of desertification and the explanatory power of the influencing factors on the spatial differentiation of the flash flood hazard, and vice versa. The grading mode was determined according to statistical rules (e.g., equidistant spacing, natural spacing, interquartile spacing, geometric spacing, and standard deviation spacing), and the number of discontinuities was set from three to eight. The OPGD model was spatially discretized by selecting the parameter combination with the highest q-value (grading mode and number of discontinuities) to detect the spatial hierarchical heterogeneity of desertification and the explanatory power of the influencing factors for the spatial variability of flash floods. Interaction detection was then used to analyze the influence of climate and terrain factors on desertification.

Factor Discretization

The optidisc function was run in the GD package, and the algorithm automatically calculated the optimal method and classification. For each continuous factor, the q-value was calculated using five different discretization methods (equidistant, natural breakpoint, quartile, geometric interval, and standard deviation methods) and different numbers of breaks, and the parameter combination with the highest q-value was selected (grading method and number of breaks). Because the number of interruptions is best classified within ten, 5-8 classes were initially set as the interval of interruptions [16]. Taking annual precipitation and average annual temperature discretization as an example, for annual precipitation, the q-value was the largest when the classification method was equally spaced and the number of classifications was eight (Fig. 2a)). Therefore, the equal spacing method was chosen to divide the annual precipitation into eight classes (Fig. 2b)). The interquartile spacing classification was chosen to divide the average annual temperature into seven classes (Fig. 2c) and 2d)). The other factors were discretized using the same principle.

Results

Characteristics of the Temporal Distribution of Desertification

During the past 20 years, the desertified area of Hulunbuir Grassland showed a decreasing trend, then increased, and then decreased again, with gradual decreases in heavy desertification and the degree of desertification. The desertification of Hulunbuir Grassland has been effectively managed, and the overall trend is decreasing (Fig. 3), with the desertified area decreasing by 296.89 km². From 2000-2005, the desertified area showed a decreasing trend, with a net decrease of 2,252.63 km², with an increase in non-deserted and heavily desertified land and a decrease in the area of mildly and moderately desertified land. From 2005-2010, the desertified area showed a net increase of 8,673.83 km², with decreases in non-deserted and mildly desertified land. From 2005-2010, the net increase in desertification area was 8673.83 km², the non-desert area decreased, and the areas of mild, moderate, and heavy desertification increased, indicating that a large area of non-desertified land developed into desertified land and that desertification developed during this period. In contrast, from 2010-2020, the net decrease in desertification area was 6718.09 km², non-desertified and mildly desertified land areas increased, moderately and heavily desertified land areas decreased, and desertification showed a reversed trend. By the end of the study period, non-desertification and mild desertification dominated the study area, with an area share of 66.11%.

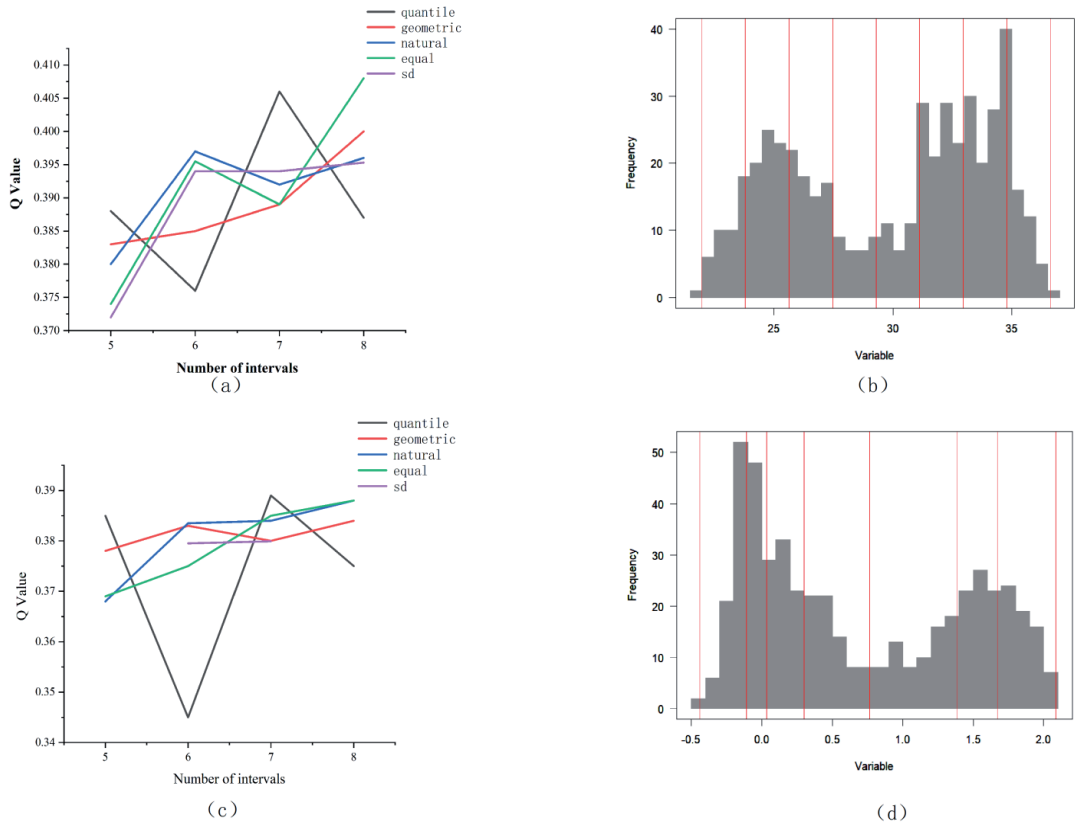

Fig. 2. Discretization of continuous factors: a) annual precipitation classification, b) optimal interval of annual precipitation, c) direction of annual mean temperature classification, and d) optimal interval of annual precipitation.

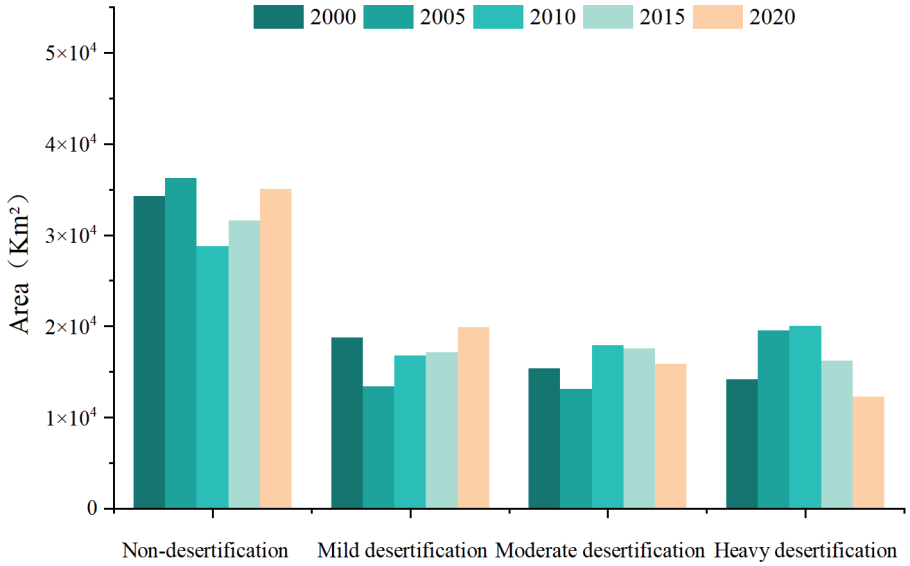

Fig. 3. Temporal distribution of desertification.

According to statistics, the area of desertification intensification from 2000-2020 was 13,824.24 km², and the area of desertification reversal was 18,240.49 km². As shown in Fig. 4, only 18% of the non-desertified land had been transformed, of which 16% had been transformed into mild desertification and 2% into moderate desertification. Of the mild desertification, 75% was transformed, and the area of desertification intensification (51%) was higher than that of desertification reversal (24%). Moderate desertification was observed in 62% of the land, of which 33% was characterized by intensification of desertification (to heavy desertification) and 29% by reversal of desertification (non-desertification or mild

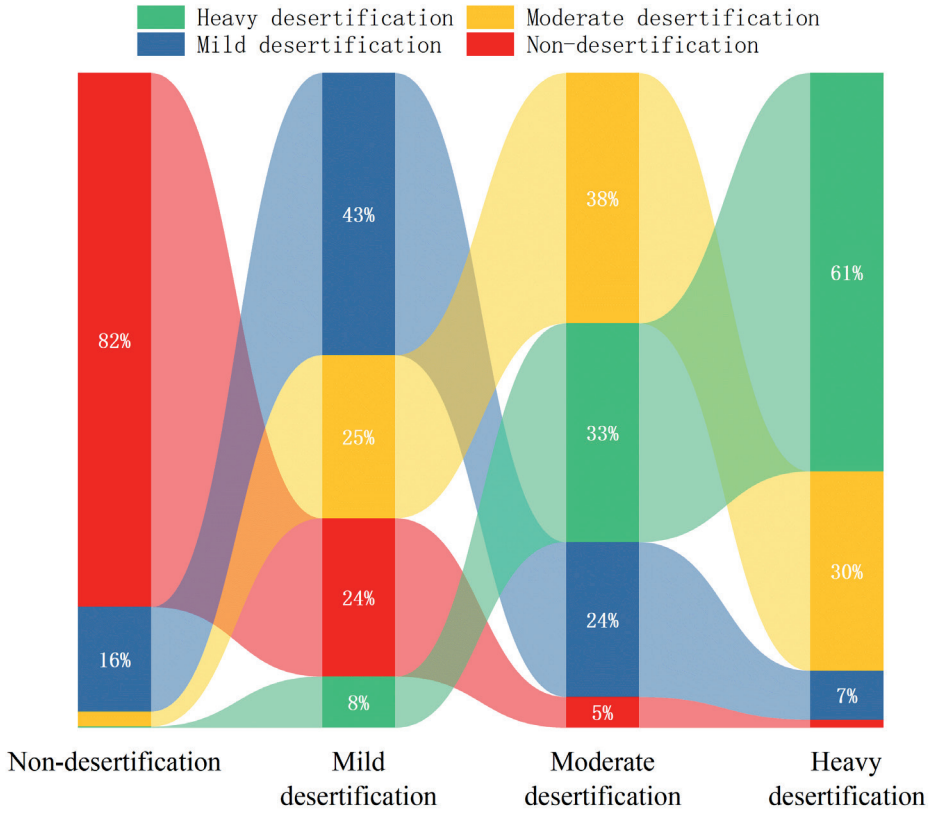

Fig. 4. Direction of desertification gravity migration.

desertification). Of the land with heavy desertification, 39% transformed, all showing a reversal of desertification (non, mild, and moderate desertification). When the Hulunbuir Sand Management Plan (2009-2013) was implemented, Hulunbuir City carried out a large-scale sand control operation. The comprehensive sand management project achieved obvious results, with the ecological environment in the project area significantly improving and forest and grass vegetation growing luxuriantly, effectively curbing the momentum of desertification of the grasslands and the desertified land being effectively managed.

Characteristics of Desertification Spatial Distribution

According to the historical desertification distribution of the county unit, New Barag Left Banner (referred to as New Left Banner) and the New Barag Right Banner (referred to as New Right Banner) were desertification-prone areas (Fig. 5a)). The global Moran's I of desertification at the county unit was 0.582 ($P<0.01$), presenting a strong spatial agglomeration, and the global Moran's I of desertification at the 500×500-m grid scale was 0.794, showing higher spatial agglomeration than that at the county scale. Among the areas with high desertification, the grid unit of New Right Banner formed an obvious high-high agglomeration within the grid unit, and the middle and southern parts of New Left Banner formed an obvious high-high agglomeration, with sporadic occurrence of low-high agglomeration. The frequency of desertification in Chen Barag Banner (referred to as Chen Banner), Ewenki Autonomous Banner (referred to as Ewenki), and Hailar was small, and the eastern part of the area formed a contiguous low-low agglomeration (Fig. 5b)).

Overall, Hulunbuir Grassland was mainly characterized by moderate desertification, which was more serious in the west than in the east, showing a trend of expansion from west to east. New Right Banner and New Left Banner had the largest desertification areas, mainly dominated by moderate and heavy desertification, showing a trend of spreading from east to east (Fig. 6). At the beginning of the study period, mild desertification was concentrated in Ewenki, Chen Banner, and New Left Banner, and with the reversal of moderate and heavy desertification, it was sporadically distributed in New Right Banner, Manzhouli, and other flag counties. Overall, mild desertification was interspersed with non-, moderate, and heavy desertification, and the area of mild desertification was gradually increasing. Moderately desertified land was distributed in the territory of each flag county and was mainly concentrated in New Left Banner, New Right Banner, and Ewenki. Heavily desertified land was mainly distributed at the edges of Lake Hulun and the three sand belts.

The centers of gravity of mild, moderate, and heavy desertification of Hulunbuir Grassland were distributed sequentially from northeast to southwest in the study

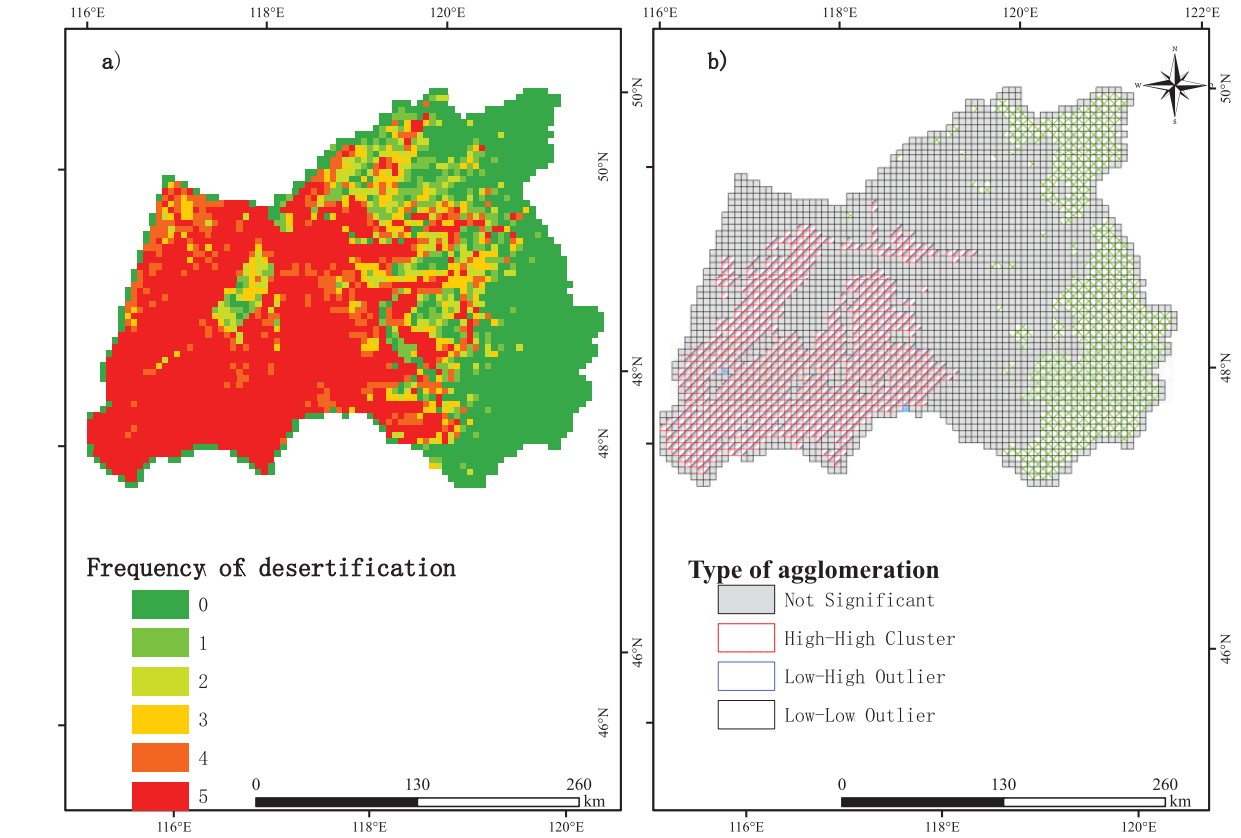

Fig. 5. Hulunbuir Sandy Land grid unit. a) Desertification frequency map, b) LISA map.

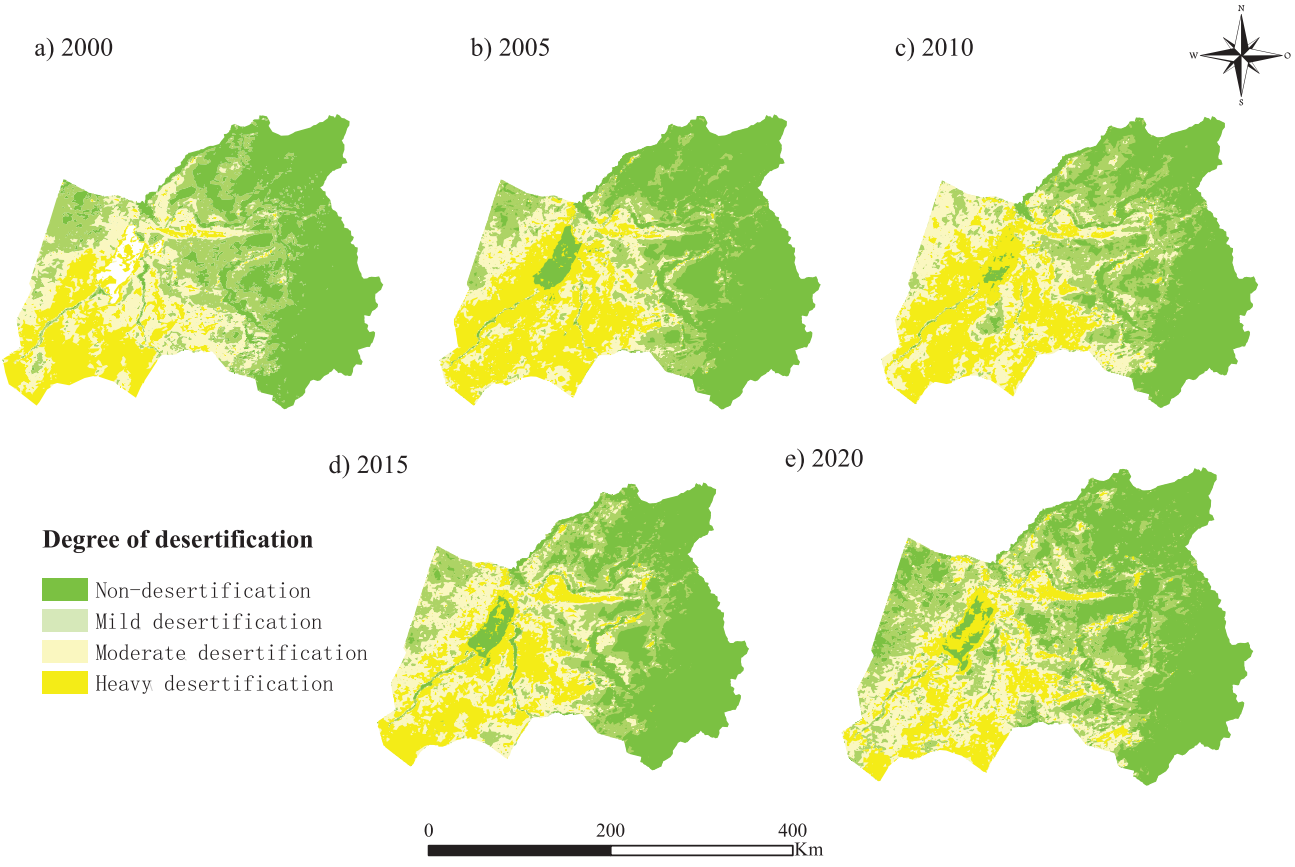

Fig. 6. Spatial and temporal distributions of desertification in Hulunbuir Sandy Land.

area. The center of gravity of mild and moderate desertification migrated along the northeast–southwest direction (Fig. 7a) and 7b)). In 2009, Hulunbuir Municipality released and implemented the "Hulunbuir Sandland Governance Plan (2009-2013)", which significantly affected mild and moderate desertification management, making 2010 an important turning point. Before 2010, mild and moderate desertification migrated to the northeast, and scattered sands appeared in the northeastern part of the study area and expanded further. After 2010, mild and moderate desertification migrated to the southwest, indicating that actions to control desertification in Hulunbuir significantly affected vegetation recovery in mild and moderate desertification areas in the northeastern part of the study area. The center of gravity of heavy desertification was consistently located in the territory of Xinyu Banner, and from 2000-2015, owing to desertification management and the effective restoration of vegetation in Xinyu Banner, the center of gravity of desertification migrated to the northeast; after 2015, the center of gravity migrated to the west.

Desertification is a Driving force in Hulunbuir Grassland

Precipitation over the last 20 years has generally shown a fluctuating upward trend (Fig. 8). From 2000-2010, the fluctuation in precipitation was small; from 2010-2015, precipitation decreased and reached its lowest value in 2015. Precipitation increased from 2015-2020. The long-term temperature change trend was not significant; starting from 2005, temperature fluctuation was frequent, and the temperature reached its minimum in 2010 and peaked in 2015. In 2016, the Hulunbuir grassland suffered from extreme weather, with precipitation reduced by 85% and the maximum temperature reaching 44.1°C, breaking the temperature record and resulting in widespread vegetation death, impeding the sand control process. Overall, annual precipitation was negatively correlated with annual average temperature (Fig. 8).

The explanatory power of single factors for desertification was identified using factor detection of the parameter-optimal geoprobe (Fig. 9a)). The explanatory power of all factors, except annual precipitation and mean annual temperature, was < 0.1. Overall, the average q-value of meteorological factors was 0.3979, and that of topographical factors was 0.0240, indicating

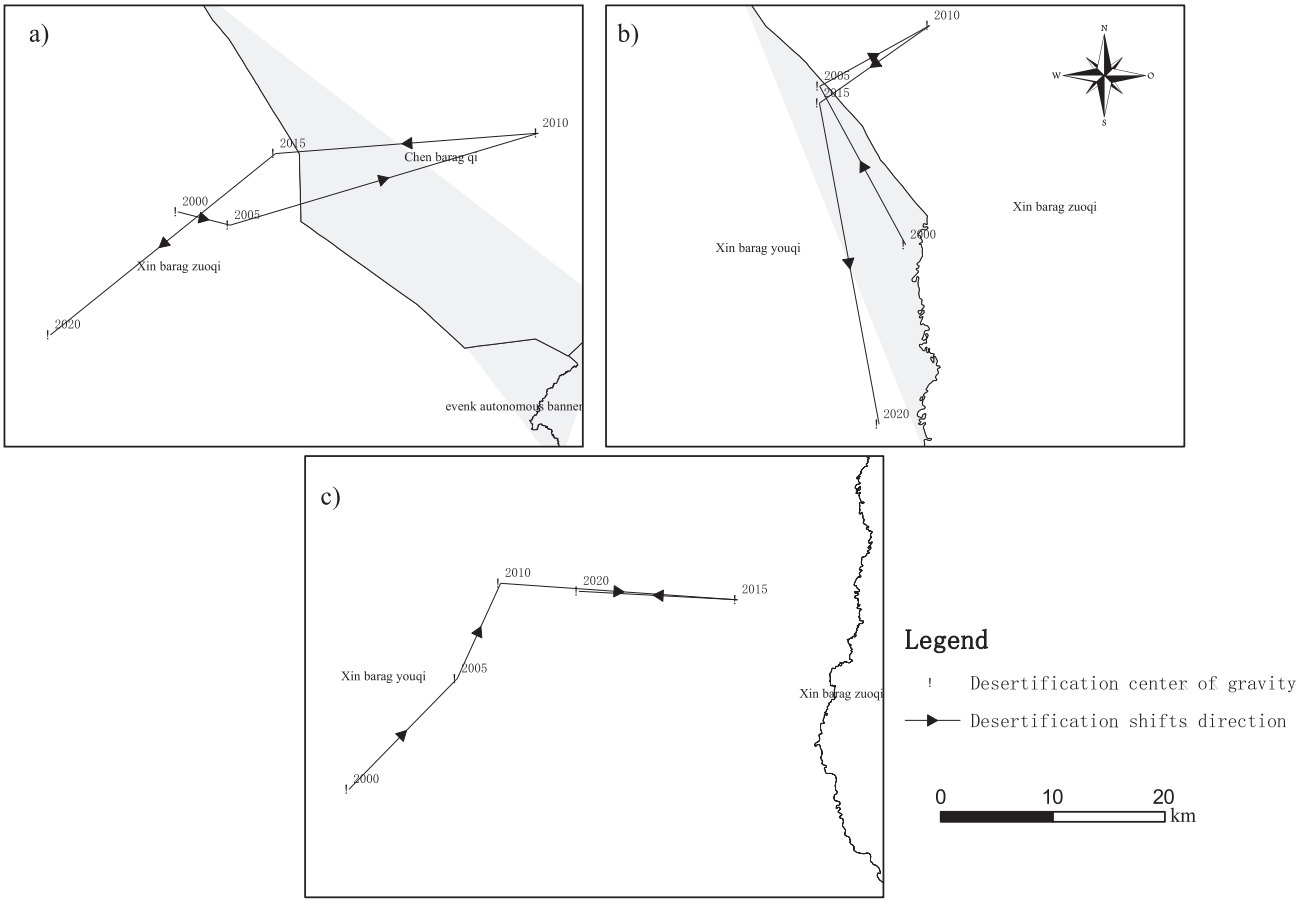

Fig. 7. Migration and change of the center of gravity of desertification in Hulunbuir Sandy Land: a) mild desertification, b) moderate desertification, c) heavy desertification.

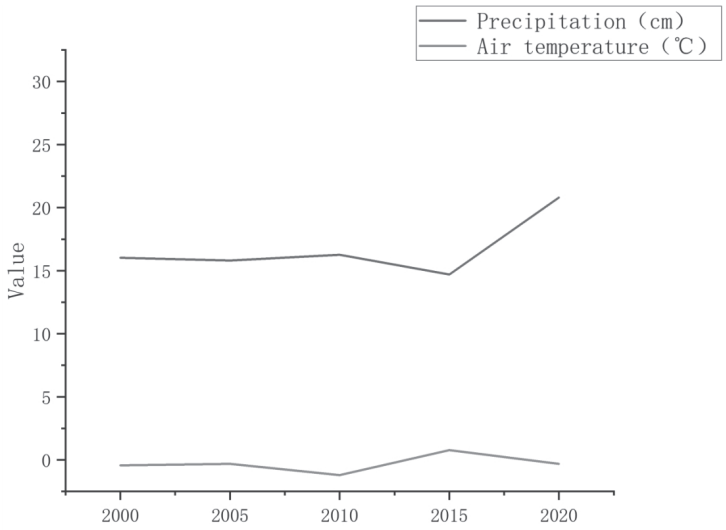

Fig. 8. Precipitation and temperature trends in Hulunbuir Grassland in the past 20 years.

that the explanatory power of meteorological factors was significantly higher than that of topographical factors, with annual precipitation (0.407) > mean annual temperature (0.389) in the explanatory power of meteorological factors. The explanatory power of topographic factors was relatively low and decreased in the following order: slope > distance from water bodies > distance from settlements > soil moisture > elevation > distance from roads > slope direction. The explanatory power of the slope direction factor was < 0.01. The P-values of the explanatory power of all factors were < 0.01, and the results of the detections were all significant. The factor detection results showed that meteorological factors played a dominant role in the desertification of Hulunbuir Grassland; in particular, annual precipitation had a stronger explanatory power for desertification, and the single-factor explanatory power of topographic factors was relatively weak.

Drivers of desertification are independent and interact strongly with each other. A total of 45 pairs of interaction combinations existed between any two factors in this study, and an interaction detector was applied to explore the combined effects of these factors on desertification in Hulunbuir Grassland (Fig. 9b)). The results of the interaction probe showed that the interactions of all factors were bivariate-enhanced, and the explanatory power (q-value) of the interaction between any two factors for desertification was greater than that of any individual factor (Fig. 9b)). Among them, the interaction between annual precipitation and distance from water bodies had the strongest explanatory power (q-value = 0.4912), indicating that the coupling of these factors could explain 50.87% of desertification, particularly considering that precipitation during the summer vegetation growth period (June–August) had higher explanatory power for

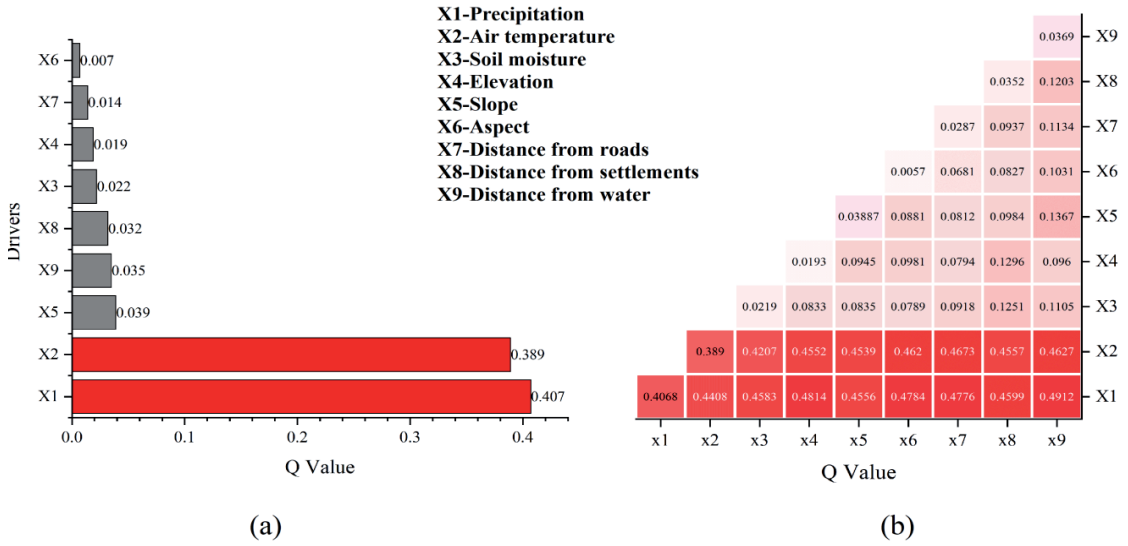

Fig. 9. Desertification driver detection results, a) factor detection results, b) interaction heat map.

desertification changes. Annual precipitation and mean temperature were enhanced by two factors (q-value = 0.4408), and the meteorological and topographic factors were nonlinearly enhanced (q-values from 0.4207-0.5087). The interaction between different topographic factors was not evident, and the distance to the road and distance to the water body had the strongest explanatory power (q-value = 0.0933), which was higher than that of the single factors of distance to the road and distance to the water body. Although individual terrain factors did not significantly affect desertification, the explanatory power was nonlinearly enhanced when interacting with meteorological factors, indicating that specific terrain conditions encountered during drought and high temperatures would significantly exacerbate desertification.

Discussion

With the social economy's growth, desertification in Inner Mongolia has become more prominent. Supported by national projects like the "Three-North" program, grass-animal balance regulations, and afforestation initiatives, desertification has been curbed, and the ecological environment has improved. As the sandy land with the best background conditions in China, Hulunbuir Sandy Land is an important ecological security barrier in northern China, and its comprehensive management has been included in the national special planning.

This study analyzes remote sensing images from 2000-2020 using ENVI, RStudio, and ArcGIS software. It shows that desertification in the region has significantly decreased over the past two decades, indicating an improving trend. The results align with previous studies on desertification's extent and spatial distribution [15, 17]. The study also identifies factors influencing desertification through a geographic detector, focusing on meteorological and topographical conditions.

Desertification in Hulunbuir has been most severe in New Left and New Right Banners, influenced by poor soil, extreme climate (low rainfall, high temperatures), and overgrazing. In 2016, extreme weather exacerbated desertification, with record low rainfall and high temperatures. The region's seasonal water deficit further strained vegetation growth and soil moisture retention, leading to intensified desertification. Significant drivers of desertification are annual precipitation and temperature, as well as steep slopes, which accelerate desertification under similar climatic conditions [18].

However, uncertainties remain, including climate change's potential to worsen desertification [19], human activities like overgrazing[20], and ongoing desertification control efforts. Future research should explore socioeconomic factors and human governance to better understand and mitigate desertification's challenges.

Conclusions

By analyzing the situation of Hulunbuir Sandy Land for the last 20 years and discussing the climate and topographic factors in the study area, the following conclusions were drawn:

(1) Desertification. In general, the desertification area of Hulunbuir grassland decreased, and the degree of desertification decreased from 2000 to 2020. Spatially, the degree of desertification in the western part of the study area is greater than that in the eastern part. The desertification of Hulunbuir grassland shows a positive spatial correlation between grid points, and there is a clustering phenomenon in local areas. Xinzuo Banner and Xinyou Banner are areas with a high degree of desertification. The forward analysis of the center of gravity in five periods found that the longitudinal influence of mild and severe desertification is greater than the latitudinal influence, while the opposite is true for moderate desertification.

(2) From the results of the detection of desertification driving forces, meteorological factors have greater explanatory power for the spatial variation of desertification than topographic factors, among which annual precipitation has the strongest explanatory power. Meteorological factors are the dominant factors for desertification in Hulunbuir grassland, and the explanatory power of topographic factors is relatively weak. When meteorological factors interact with topographic factors, the explanatory power shows nonlinear enhancement, indicating that desertification is further intensified under the dual drive of meteorology and topography.

Acknowledgments

This study was funded by the Inner Mongolia Science and Technology Program (2022YFDZ0055).

Conflict of Interest

The authors declare no conflict of interest.

References

1. LYU Y.L., SHI P.J., HAN G.Y., LIU L.Y., GUO L.L., HU X., ZHANG G.M. Desertification control practices in China. Sustainability. **12** (8), 3258, **2020**.
2. YIWEN H., ZONG L., XUEQIAN Y., JIAYING W. Desertification monitoring and early warning in context of sandy land consolidation .Transactions of the Chinese Society of Agricultural Engineering. **33** (10), 271. **2017**.
3. ZHANGNING X., WEI L., JIANGHU L., YINGXIN W., ZHENGUO W. Monitoring and assessment of desertification reversal in ecologically fragile areas: A case study of the Mu Us Sandy Land. Journal of environmental management. **373**, 123695, **2024**.

4. WANLI S., FEISHENG F., KE Y., YONG Z., JIQIANG Z., JIE S. Water Chemical Characteristics and Safety Assessment of Irrigation Water in the Northern Part of Hulunbeier City, Grassland Area in Eastern China. Sustainability. **14** (23), 16068, **2022**.
5. QIUYING Z., XIAOSHENG H., PING W., MING L., YI DI., YUXUAN W., TIANTIAN P., WENJIE L., XIAO G., XIAOMING S., JUNSHENG L. Estimation, Spatiotemporal Dynamics, and Driving Factors of Grassland Biomass Carbon Storage Based on Machine Learning Methods: A Case Study of the Hulunbuir Grassland. Remote Sensing. **16** (19), 3709, **2024**.
6. DE OLIVEIRA BARROS K., ALVARES SOARES RIBEIRO C.A., MARCATTI G.E., LORENZON A.S., MARTINS DE CASTRO N.L., DOMINGUES G.F., ROMÁRIO DE CARVALHO J., ROSA DOS SANTOS A. Markov chains and cellular automata to predict environments subject to desertification. Journal of Environmental Management. **225**, 160, **2018**.
7. ZHANG Q., TANG H.P., CUI F.Q., DAI L.W. SPEI-based analysis of drought characteristics and trends in Hulun Buir grassland. Acta Ecologica Sinica, **39** (19), 7110, **2019** [In Chinese].
8. KARAVITIS C.A., TSESMELIS D.E., OIKONOMOU P.D., KAIRIS O., KOSMAS C., FASSOULI V., RITSEMA C., HESSEL R., JETTEN V., MOUSTAKAS N., TODOROVIC B., SKONDRAS N.A., VASILAKOU C.G., ALEXANDRIS S., KOLOKYTHA E., STAMATAKOS D.V., STRICEVIC R., CHATZIGEORGIADIS E., BRANDT J., GEESON N., QUARANTA G. A desertification risk assessment decision support tool (DRAST). Catena. **187**, 104413, **2020**.
9. YANG J., HUANG X. The 30 m annual land cover dataset and its dynamics in China from 1990 to 2019. Earth System Science Data, **13** (8), 3907, **2021**.
10. WANG S.X. Research on desertification grade evaluation based on multi-source data. Shandong University of Technology. **2022** [In Chinese].
11. FENG K., YAN C.Z., XIE J.L., QIAN D.W. Spatial-temporal evolution of aeolian desertification process in Ordos City during 1975-2015. Chinese Journal of Deserts. **38** (2), 233, **2018** [In Chinese].
12. WANG J.F., XU C.D. Geoprobes: Principles and prospects. Journal of Geography. **72** (1), 116, **2017** [In Chinese].
13. SONG Y.Z., WANG J.F., GE Y., XU C.D. An optimal parameters-based geographical detector model enhances geographic characteristics of explanatory variables for spatial heterogeneity analysis: cases with different types of spatial data. GIScience & Remote Sensing. **57** (5), 593, **2020**.
14. JIN K., WANG F., HAN J.Q., SHI S.Y., DING W.B. Impacts of climate change and human activities on vegetation NDVI changes in China from 1982 to 2015. Journal of Geography. **75** (5), 961, **2020** [In Chinese].
15. ZHANG T.Q., YANG G., LIU F., MU Q.E., TAO L., MA Y. Land use change and ecological service value in Hulunbuir sandland from 2000 to 2020. Soil and Water Conservation Bulletin, **41** (4), 331, **2021** [In Chinese].
16. ZHANG R.J., CHEN Y.H., ZHANG X.X., FANG X.Q., MA Q., REN L.L. Spatial-temporal pattern and driving factors of flash flood disasters in Jiangxi Province analyzed by optimal parameters-based geographical detector. Geography and Geo-Information Science, **37** (4), 72, **2021** [In Chinese].
17. NA R.S. Characterization of spatial and temporal changes of land desertification in Hulunbuir Sandland. Inner Mongolia Normal University. **2018** [In Chinese].
18. ROY P., PAL S.C., CHAKRABORTTY R., CHOWDHURI I., SAHA A., RUIDAS D., ISLAM A.R.M.T., ISLAM A. Climate change and geo-environmental factors influencing desertification: a critical review. Environmental Science and Pollution Research International. **2024**.
19. LI J., ZHANG C.L., LI Q., SHEN Y.P., JIA W.R., TIAN J.L. Research on vegetation dynamics in sandy land ecosystems. Journal of Beijing Normal University (Natural Science Edition). **53** (3), 323, **2017** [In Chinese].
20. SIMPLÍCIO A.A.F., COSTA C.A.G., NAVARROHEVIA J., CARLOS D.A.J. Erosion at hillslope and micro-basin scales in the Gilbués desertification region, Northeastern Brazil. Journal Land Degradation & Development. **32** (3), 1487, **2020**.